Numerical Analysis on Hydraulic Power Take-Off for Wave Energy Converter and Power Smoothing Methods

Preprint

Yi-Hsiang Yu, Nathan Tom, and Dale Jenne
National Renewable Energy Laboratory

Presented at the 37th International Conference on Ocean, Offshore, and Arctic Engineering (OMAE2018)
Madrid, Spain
June 17–22, 2018

NOTICE

Cover Photos by Dennis Schroeder: (left to right) NREL 26173, NREL 18302, NREL 19758, NREL 29642, NREL 19795.

NREL prints on paper that contains recycled content.

NUMERICAL ANALYSIS ON HYDRAULIC POWER TAKE-OFF FOR WAVE ENERGY CONVERTER AND POWER SMOOTHING METHODS

Yi-Hsiang Yu*
National Renewable Energy Laboratory
Golden, CO, USA
Email: yi-hsiang.yu@nrel.gov

Nathan Tom
National Renewable Energy Laboratory
Golden, CO, USA
Email: nathan.tom@nrel.gov

Dale Jenne
National Renewable Energy Laboratory
Golden, CO, USA
Email: dale.jenne@nrel.gov

ABSTRACT

One of the primary challenges for wave energy converter (WEC) systems is the fluctuating nature of wave resources, which require the WEC components to be designed to handle loads (i.e., torques, forces, and powers) that are many times greater than the average load. This approach requires a much greater power take-off (PTO) capacity than the average power output and indicates a higher cost for the PTO. Moreover, additional design requirements, such as battery storage, are needed, particularly for practical electrical grid connection, and can be a problem for sensitive equipment (e.g., radar, computing devices, and sensors). Therefore, it is essential to investigate potential methodologies to reduce the overall power fluctuation while trying to optimize the power output from WECs. In this study, a detailed hydraulic PTO model was developed and coupled with a time-domain hydrodynamics model (WEC-Sim) to evaluate the PTO efficiency for WECs and the trade-off between power output and fluctuation using different power smoothing methods, including energy storage, pressure relief mechanism, and a power-based setpoint control method. The study also revealed that the maximum power fluctuation for WECs can be significantly reduced by one order of magnitude when these power smoothing methods are applied.

KEYWORDS

Renewable energy; wave energy converter; power take-off (PTO); hydraulic PTO; power-based setpoint control

---

*Address all correspondence to this author.

INTRODUCTION

Studies have shown that extracting energy from ocean wave resources has the potential to provide a significant contribution to the electricity supply [1]. In the past several decades, a wide variety of wave energy converter (WEC) technologies have been proposed, including oscillating water columns, oscillating body designs, and over-topping devices [2]. However, wave energy technology is still in the research and development stage. Therefore, levelized cost of energy (LCOE) for WEC designs is still high, compared to other renewable energy technologies, such as wind and solar [3].

Although the cost may gradually decrease with industrialization and mass production as large WEC farms are being developed, it is essential to find an efficient pathway to reduce costs for the WEC industry to be successful. One of the primary challenges for WECs is the fluctuating nature of waves. As a result, WEC components must be designed to handle loads (i.e., torques, forces, and powers) that are many times greater than the average load, which requires a much greater power take-off (PTO) capacity than the average power output [4]. For example, Tedeschi et al. [5] showed that the generated peak power from the WEC can be more than one order of magnitude larger than the absorbed average power. The large peak-to-average power ratio implies a much higher PTO cost for the WEC system. In addition, these fluctuations will have important implications for the stability of voltage and frequency to the grid system and can be a problem for sensitive equipment (e.g., radar, computing devices, and sensors) and will drive additional design requirements for practical utilization. Therefore, it is essential to reduce the peak-to-average power ratio while trying to maximize or at least maintain the power output from WECs by implementing energy storage/relief and advanced control methods.

1

There are many different forms of power smoothing technologies. Most commonly used are energy storage units, which depend on the types of PTO designs. For a mechanical system, such as direct-drive and gearbox designs, a flywheel or a superconducting magnetic energy storage system is often used to store energy [6]. On the other hand, a pressure accumulator can be used for a hydraulic PTO design [7]. For WEC design and power performance analysis, these energy storage units are often considered based on simplified assumptions. For example, in the Reference Model (RM) project, the analysis was conducted using a specified frequency-independent mechanical-to-electrical conversion efficiency and a 30% capacity factor to size the generator and cut off the maximum average power production [8]. However, PTO is a dynamic system, wherein the power output from the WEC depends on the size of the generator and the other subsystem and how the power smoothing methods are applied. Therefore, it is essential to model not only the hydrodynamics of the WEC but also the PTO subsystems, and to investigate potential methodologies to reduce the overall power fluctuation while trying to optimize the power output from WECs. PTO-Sim, a PTO simulator, was developed as part of the WEC-Sim model, which is a time-domain radiation-and-diffraction-method-based numerical method, to simulate different types of PTO systems for WECs [9]. However, to better understand the PTO efficiency and investigate different types of power smoothing methods, a detailed representation of the PTO that can be used to simulate its subsystem is needed.

In this study, we focus on the hydraulic PTO system. A detailed hydraulic PTO model for WEC-Sim is developed using Simscape Fluids (MATLAB). The objective of this study is to verify the PTO design specifications applied for the RM project (RM3 design [8]) using the developed numerical model and to investigate the overall WEC power generation efficiency. The trade-off between power output and the fluctuation—using different power smoothing methods—is also evaluated. The paper first describes the hydrodynamics modeling methods and the hydraulic PTO model, as well as how the control method is implemented for power smoothing. Next, we discuss a hydrodynamics validation study and the simulation of a two-body floating point absorber (FPA) WEC. The hydrodynamics model is then coupled with the hydraulic PTO model and is used to evaluate the system power output, PTO efficiency, and power output fluctuation using energy storage, the pressure relief mechanism, and an advanced control method. Finally, a discussion on the influence of using these power smoothing methods on the PTO portion of the LCOE and potential pathway for cost reduction is included.

METHODOLOGY

This section describes WEC-Sim, the time-domain model, which is used to simulate the WEC hydrodynamics, hydraulic PTO model, and the control algorithm to minimize the power output fluctuation.

Hydrodynamics

WEC-Sim is a radiation-and-diffraction-method-based numerical model that has been developed to solve the system dynamics of WECs consisting of multiple bodies, PTO systems, and mooring systems [10]. The dynamic response in WEC-Sim is calculated by solving the equation of motion for each body about its center of gravity, based on Cummins' equation [11], which can be written as

$$(m + A_\infty)\ddot{X} = -\int_0^t K(t-\tau)\dot{X}(\tau)d\tau \\ + F_{ext} + F_{vis} + F_{res} + F_{PTO} + F_{mo}$$

(1)

where A_∞ is the added mass matrix at infinite frequency, X is the (translational and rotational) displacement vector of the body, m is the mass matrix, K is the matrix of impulse response function, F_{ext}, F_{PTO}, F_{mo}, F_{vis}, and F_{res} are the vector of wave-excitation force, PTO force, mooring force, quadratic viscous drag term calculated using Morison's equation, and net buoyancy restoring force. Simulations are performed in the time domain by solving the governing equations of motion in 6 degrees of freedom for each body. In this study, we used WAMIT [12], which is a boundary-element-method-based frequency-domain potential flow solver, to obtain the added mass, wave excitation, impulse response function, and restoring stiffness terms. The PTO force was obtained from the hydraulic PTO model, which was developed using SimScape Fluids, a MATLAB toolbox that provides prebuilt libraries for modeling hydraulic systems. More details on the hydraulic model and the PTO subsystems are described in the Hydraulic PTO section.

Power-Based Setpoint Control

In this work, a power-based setpoint control was used in an attempt to reduce the peak instantaneous power in an electric generator while maintaining the same time-averaged power production over the simulated sea state. In control theory, a setpoint is the desired or targeted value for a variable of a system. The departure of the variable from this setpoint is used to regulate the system response normally through feedback. The electrical power generated by the variable-speed drive is controlled by adjusting the resistive torque through a variable-dashpot damper.

For these simulations, a proportional control algorithm was designed to generate a control signal that is proportional to the difference between the generator setpoint power and the measured instantaneous power. The setpoint power was calculated by simulating the WEC for a given sea state with the generator resistive torque equal to the product of the generator rotational speed times the torque produced by a constant viscous rotational damper. The time-averaged power calculated from this sea state was used as the setpoint power for the simulations with power control. During the power control simulations, the generator damper was increased or decreased based on the following ex-
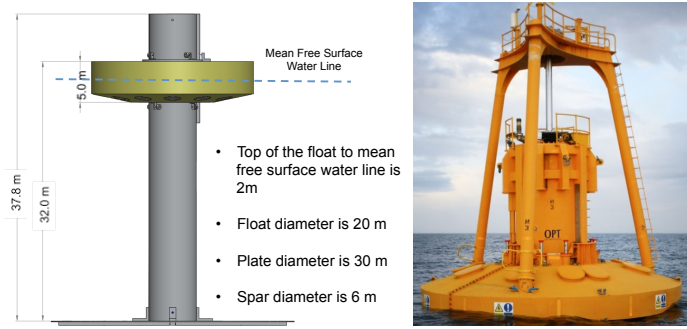
2

FIGURE 1. THE SCHEMATIC (SIDE VIEW) OF THE WEC-SIM FPA MODEL (LEFT) AND OPT'S POWERBUOY OPERATING OFF THE COAST OF SCOTLAND. PHOTO BY OPT, NREL 22857 (RIGHT)

pressures

$$e = P_i - P_{sp} \tag{2}$$

$$\hat{e} = \frac{e}{P_{sp}} \tag{3}$$

$$C_{PTO} = C_{base}(1 - G\hat{e}) \tag{4}$$

where P_i is the instantaneous generator power, P_{sp} is the setpoint power, C_{PTO} is the generator rotational damper value, C_{base} is the base generator rotational damper value when power control is not implemented, and $G > 0$ is the proportional gain that can be tuned to adjust performance. During operational deployment, it may be necessary to calculate the power setpoint either through simulations with new sea state parameters (significant wave height and peak period) or a running average calculated from the last 15, 30, or 60 min of logged performance data.

MODEL SETUP

This section describes the properties of the WEC, the WEC-Sim model, and the hydraulic PTO model.

Model and Mass Properties

A two-body FPA was simulated in this study, which is similar to Ocean Power Technologies (OPT) PowerBuoy (Fig. 1). It contains a float and a spar/plate that is connected to a central column, and it converts energy from the relative motion between the float and the spar/plate induced by ocean waves. The relative motion is in the axial direction of the device. The two-body FPA design was developed as part of the U.S. Department of Energy's RM Project [8]. The dimensions and mass properties for the WEC are presented in Fig. 1 and Table 1. The mass properties included the mass of the device and ballast and are presented in full scale. We also assumed both the float and spar/plate were located at their equilibrium positions, in which the mass for each body was equal to its displaced mass.

TABLE 1. FPA MODEL SPECIFICATIONS

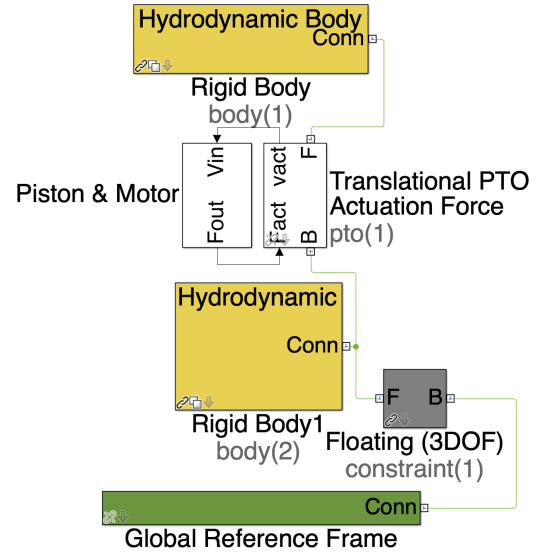|	Center of Gravity (m)	Mass (10^3kg)	Moment of Inertia (10^3kg-m^2)		
			20900	0	0
Float	[0, 0, -0.72]	727.01	0	21300	4.30
			0	4.30	31700
Spar/		137000	0	0	
Plate	[0, 0, -21.29]	878.30	0	137000	218
			0	218	28500

FIGURE 2. FPA COMPONENTS IN WEC-SIM

WEC-Sim

Based on the potential flow solution hydrodynamic coefficients, the viscous damping coefficient, given mooring stiffness, and the PTO mechanism, the time-varying forces were calculated and applied in WEC-Sim. Figure 2 shows the two-body FPA in the WEC-Sim model and blocks that contain the modules for calculating the wave radiation, excitation, net buoyancy restoring, viscous damping, and mooring forces. The float was connected to the spar/plate through a translational PTO joint, which is coupled to the hydraulic PTO model ("Piston & Motor" block), and the spar/plate was connected to the seabed using a floating joint connection[1]. The reaction PTO force in the axial direction from the hydraulic system is

$$F_{PTO_{ax}} = \Delta P_c A_c \tag{5}$$

where ΔP_c is the pressure difference from the hydraulic cylinder and A_c is the cylinder area.

---

[1] A 3-DOF joint was used instead of a 6-DOF joint because we only considered unidirectional waves in this study.
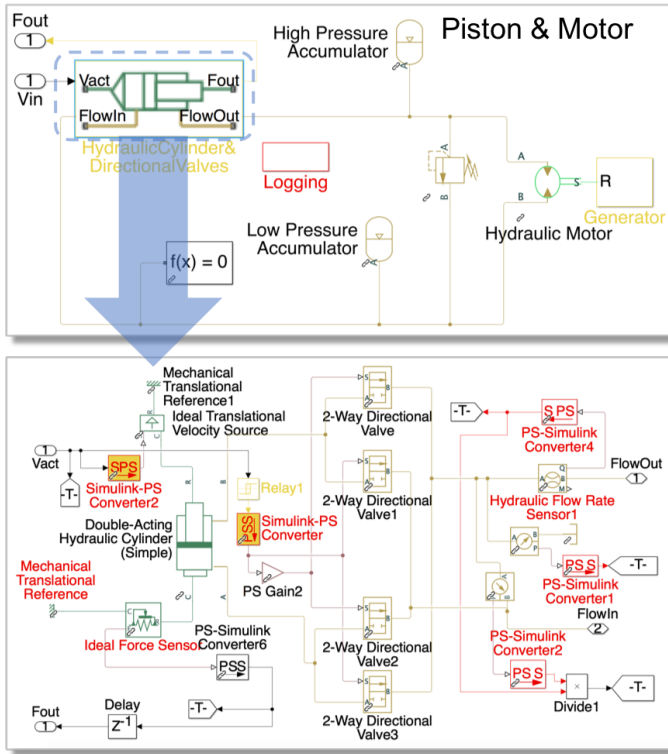
FIGURE 3. HYDRAULIC PTO COMPONENTS IN WEC-SIM

To accelerate the simulation and improve the computational efficiency, the hydrodynamics and hydraulics are simulated using different time-step sizes. The numerical model solves the 6 degrees-of-freedom equation of motion for each WEC body in the time-domain module using a fourth-order Runge-Kutta algorithm with a given fixed time-step size. On the other hand, the hydraulics are solved using a variable time-step method. The time-step size for solving the hydraulics is an order of magnitude smaller than the one used for the hydrodynamics simulations.

Hydraulic PTO

Figure 3 shows the PTO component inside the "Piston & Motor" block from the WEC-Sim model (as shown in Fig. 2). The hydraulic PTO system consists of a set of subcomponents, including a dual-acting hydraulic cylinder, directional valves, high- and low-pressure accumulators, a pressure bypass valve, and a hydraulic motor and a generator, which provides a gear speed ratio that translates the slow motion of the WEC to higher speeds at the generator.

The accumulator is used for energy storage that reduces the hydraulic fluctuation in the system, and the pressure bypass valve is designed to avoid the pressure and power generation spikes by short-circuiting the system to bypass the hydraulic motor and generator. The hydraulic motor is connected to a generator block, which includes a representation of the electrical generator and the applied controller. For simplicity, the electrical generator was represented by a rotational damper and the controller was applied to adjust resistive torque. The mechanical power, P_M, and the

electrical power, P_E, which include the losses of the hydraulic motor and generator, are given as

$$P_M = -F_{PTO_{trans}}\dot{X}_c, \tag{6}$$

$$P_E = \tau_m \omega_m \eta_g, \tag{7}$$

where $\dot{X}_c$ is the velocity of the hydraulic cylinder, τ_m is the torque from the hydraulic motor, ω_m is the angular velocity, and η_g is the electrical generator efficiency.

HYDRODYNAMICS VALIDATION

To validate the hydrodynamic model, we compared the results from the WEC-Sim simulations to those from a 1:33-scale wave tank test that was conducted at the Scripps Institute of Oceanography in San Diego, California [13]. In the validation study, the hydraulic PTO was replaced by a translational joint with a linear damper. A drag coefficient of 1 was used in surge for both the float and the spar/plate, and the values in both heave and pitch for the float and spar/plate were set to 1.1 and 3.7, respectively. Decay tests and a set of regular wave tests for different damping values were performed.

In the decay test, the WEC was placed with an initial displacement, or was initially rotated with an angle (as listed in Table 2) at full scale. Figure 4 shows the time histories of the heave, pitch, and surge decay tests obtained from the numerical simulations and experimental wave tank tests. The device was modeled in WEC-Sim with a time step of 0.05 s. The heave and pitch decay tests were conducted when the mooring was detached, and the surge decay test was performed when the model was connected to the mooring to provide surge-restoring force.

TABLE 2. DECAY TEST INITIAL DISPLACEMENT

Decay Test	Initial Displacement	Mooring
Heave	$H_{in} = -2m$	No
Pitch	$\alpha_{in} = 0.185 rad$	No
Surge	$S_{in} = 11m$	Yes

In the regular wave test, the numerical simulations were performed at full scale for regular waves with H= 3m and wave periods, T, ranging from 8 to 18 s, with a time step of 0.08–0.18 s, depending on the period, and PTO damping values of 2,250 kNs/m and 7,000 kNs/m. The numerical simulation results were compared to two sets of experimental wave tank test measurements. The power output is plotted against the incoming wave frequency in Fig. 5, where the power output is represented by capture width[2]. The averaged power was calculated by integrating the instantaneous power over time, after the transient response had damped out and only the steady-state response

---

[2]Capture width=P/J, where P is power, and J is wave energy flux (in kW/m), with J= $g^2 T H^2/(32\pi)$ for linear deep-water waves.
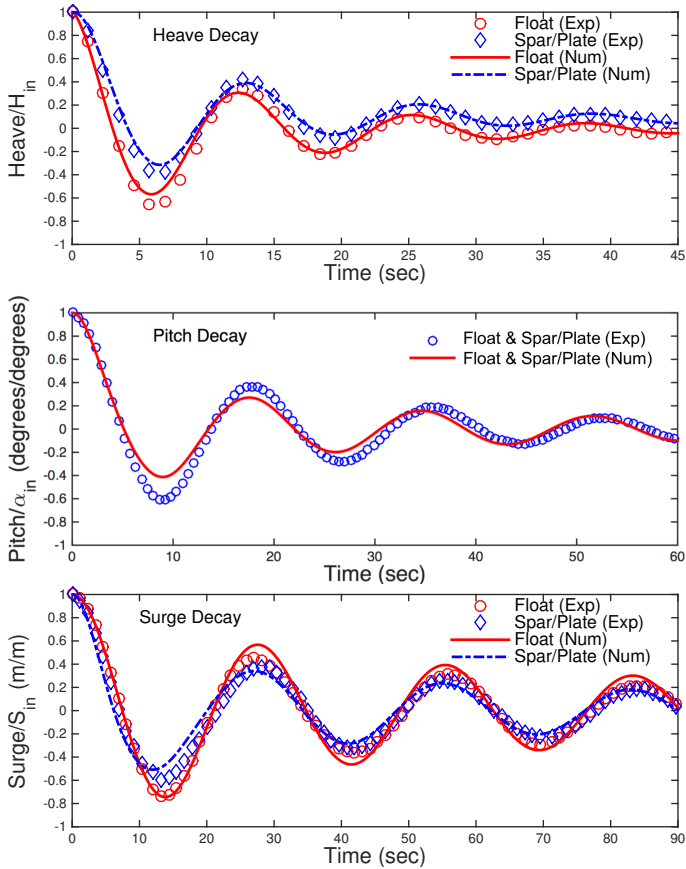
4

FIGURE 4. THE TIME HISTORIES OF THE RESPONSES AT THE MODEL CENTER OF GRAVITY (SCALED BY INITIAL DISPLACEMENT) IN THE HEAVE, PITCH, AND SURGE DECAY TESTS FOR THE FLOAT AND SPAR/PLATE FROM WEC-SIM SIMULATIONS AND EXPERIMENTS

FIGURE 5. POWER OUTPUT IN REGULAR WAVES WITH H=3m AND T=8-18s FROM WEC-SIM SIMULATIONS AND EXPERIMENT MEASUREMENTS

TABLE 3. SELECTED WAVE ENVIRONMENT

Wave #	Tp (s)	Hs (m)	Weighting
IWS 1	7.31	2.34	0.175
IWS 2	9.86	2.64	0.268
IWS 3	11.52	5.36	0.058
IWS 4	12.71	2.05	0.295
IWS 5	15.23	5.84	0.034
IWS 6	16.50	3.25	0.054

remained. we estimated the tank test PTO damping coefficient based on the average power and the average relative motion amplitude, assuming the system was linear [13]. Overall, the simulation results agreed well with those from the experimental data for both the decay and regular wave tests.

RESULTS

Irregular wave statistics data are often given in terms of the joint probability distribution and typically represented by the percentage occurrence of each binned sea state. For simplicity and to limit the required number of simulations, we follow the approach used in the Wave Energy Prize [14], in which only six sea states were considered. The six sea states are listed in Table 3, where the adjusted weighting function is given based on the wave environment for Newport, Oregon, which has an estimated annual averaged energy flux of 37.9 kW/m [14]. This section describes how the PTO parameters were determined, the influence on the power performance and fluctuation using different power smoothing methods, and the overall efficiency of the WEC under different sea states.
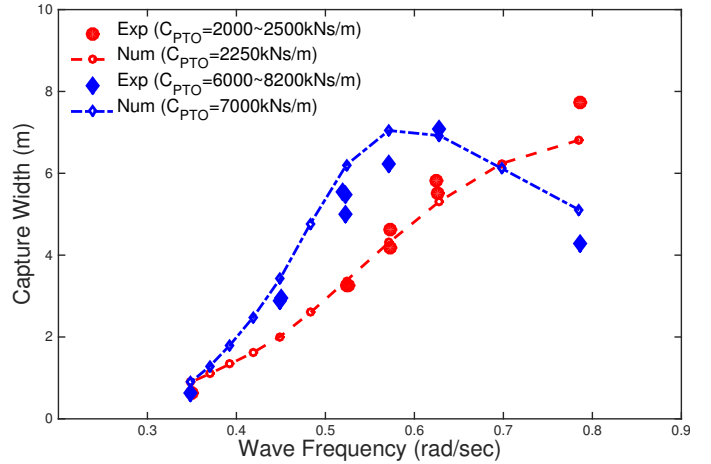
Hydraulic PTO Parameters

The PTO parameters are listed in Table 4. The hydraulic piston area was determined based on the simulated PTO force and a targeted pressure drop of 2.5×10^4 kPa in the hydraulic system for IWS5. The PTO force was obtained by simulating the WEC with a linear damper and a passively controlled damping coefficient, which resulted in an average PTO force of 1.5×10^3 kN. The other parameters were selected by designing the system for IWS2. The accumulator precharge pressure was selected to maximize the accumulator efficiency but also to keep the system's operating hydraulic pressure within a reasonable range. The hydraulic motor displacement and the rotational damper value were adjusted to maximize the WEC power output, while maintaining an average shaft speed of 1,800 rpm and considering an overall generator efficiency of 95%. In this study, the same motor displacement was applied to all of the cases, and only the damper value was adjusted to keep an average shaft speed of 1,800 rpm for different sea states and when different power smoothing methods were applied. Note that the PTO parameter optimization is beyond the scope of this work. A design optimization study is most likely going to improve the overall WEC power performance as well as the application of a variable

5

TABLE 4. HYDRAULIC PTO PARAMETERS

Parameter	Value
Hydraulic cylinder piston area	0.06 m^2
Valve passage maximum area	0.01 m^2
Accumulator precharge pressure	3.5×10^3 kPa
Hydraulic motor displacement	$3.5 \times 10^{-5} \text{m}^3/\text{rad}$
Volumetric efficiency	92%
Friction torque vs. pressure drop	0.6×10^{-6}
Generator efficiency	95%

displacement motor or other advanced control methods, particularly for the off-design wave environment. Based on selected parameters, the hydraulic PTO has an efficiency (ratio between P_E and P_M) ranging between 74% and 80%, depending on the power smoothing methods, for the designed operational sea state (IWS2).It should be noted that the hydraulic efficiency is calculated using the default loss terms defined in Simscape Fluids for both leakage (volumetric efficiency) and frictional losses (mechanical efficiency) for each component within the PTO. Additionally the dynamics of the valves have been assumed negligible along with the inertia effects of the hydraulic fluid. Therefore it is likely that a real-world PTO would have a lower efficiency, although we do not anticipate a significant variance from the 74-80% value calculated in the model.

Hydraulic Accumulator

The hydraulic PTO is a closed-loop system that includes a high-pressure accumulator and a low-pressure accumulator. The high-pressure accumulator is used for energy storage to smooth the power output, and the low-pressure accumulator is used to re-energize the hydraulic fluid. The influence of the pressure accumulator was first investigated by performing a series of simulations using different sizes of the accumulator, ranging from 0.5 m^3 to 8 m^3, in which the size of the accumulator is referring to the volume of one accumulator. For simplicity, we assume the high-pressure and low-pressure accumulators have the same settings (e.g., size and precharge pressure). To evaluate the variation of system power output, we calculate the power fluctuation ratio as

$$R_{PF} = \frac{\Delta P_E}{P_{avg}} = \frac{P_{max} - P_{min}}{P_{avg}} \quad (8)$$

where the maximum and minimum values are calculated using 99.9 and 0.1 percentiles of identified peaks from the simulated time history.

Figure 6 plots the time history from the WEC-Sim simulations using different sizes of the accumulator, and Figure 7 shows the influence on power output fluctuation. The pressure
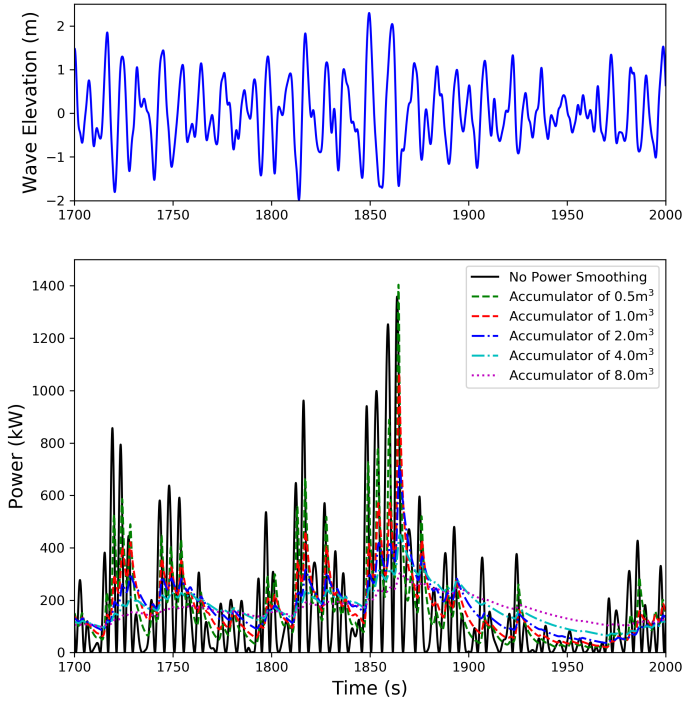

FIGURE 6. INFLUENCE OF CHANGING THE VOLUME OF THE ACCUMULATOR ON INSTANTANEOUS POWER OUTPUT: (TOP) TIME HISTORY OF THE WAVE ELEVATION; (BOTTOM) TIME HISTORY OF THE ELECTRICAL POWER OUTPUT
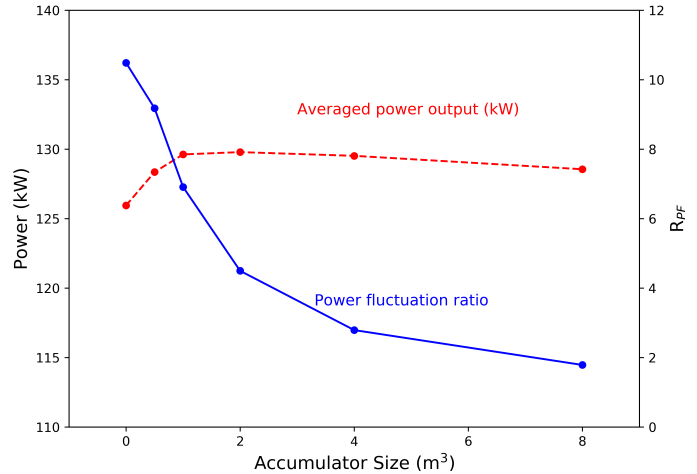

FIGURE 7. INFLUENCE OF CHANGING THE SIZE OF THE ACCUMULATOR ON POWER OUTPUT AND ITS FLUCTUATION

accumulator is effective to smooth the power output by avoiding P_{min} goes to zero, and R_{PF} is reduced from 10 to 1.8, with a 3% change in power output. However, it is less effective for reducing the spikes, unless a very large accumulator is used. In addition, the cost and the space needed to install a large accumulator must be considered for practical applications. As a result, we chose an accumulator with a volume of 1 m^3 ($R_{PF} = 6.9$) for the following analyses, which was the size of the accumulator used for the FPA WEC design in the RM project [8].
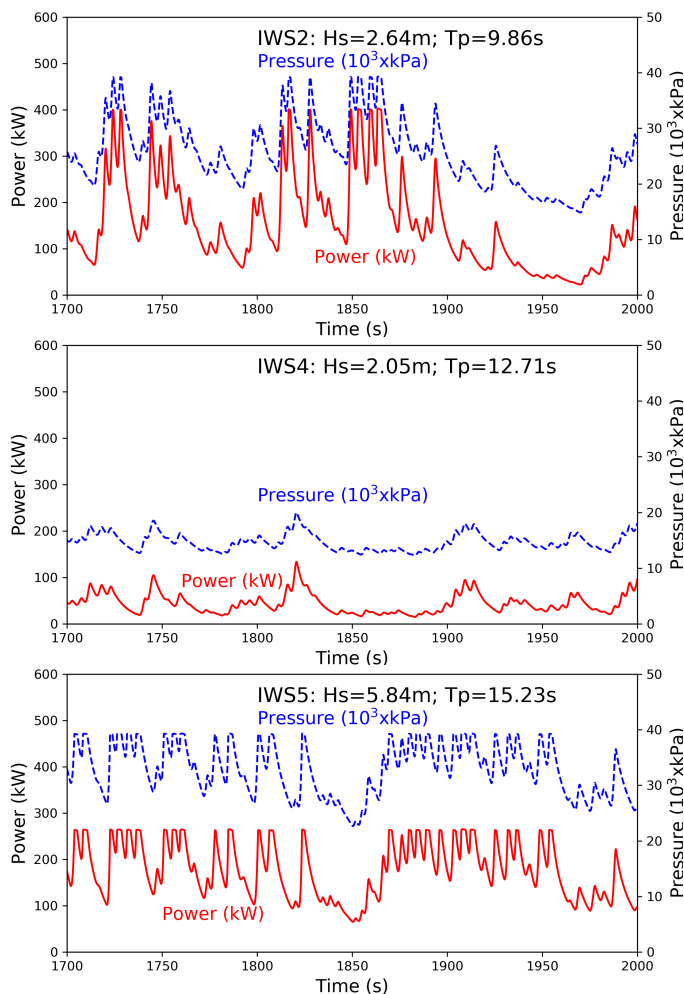
6

FIGURE 8. TIME HISTORIES OF THE POWER OUTPUT AND SYSTEM HYDRAULIC PRESSURE USING BOTH THE ACCUMULATOR (1m^3) AND PRESSURE BYPASS VALVE

Pressure Bypass Valve

The hydraulic components, such as the pipe, cylinder, and motor, are often designed to operate below a specific pressure value (e.g., 6,000 psi, which is 4.14×10^4 kPa) to maintain their reliability with a reasonable cost. As a result, the fluctuation in pressure can be another design challenge for the hydraulic PTO system. Using a pressure bypass valve is one of the most straightforward approaches to mitigating pressure and power generation spikes. It was used here to bypass the hydraulic motor and generator when the "pressure difference" went beyond a threshold limit.

We set the valve pressure difference equal to 3.45×10^4 kPa to keep the maximum hydraulic pressure in the system slightly below 4×10^4 kPa. The influence of using the pressure bypass valve on the fluctuation of pressure and power output was investigated. The simulated results are plotted in Fig. 8. Note that the accumulator (1 m^3) was also included in the simulations. The pressure bypass valve was very effective in mitigating the spikes of power output and pressure. By controlling the upper limit of the hy-
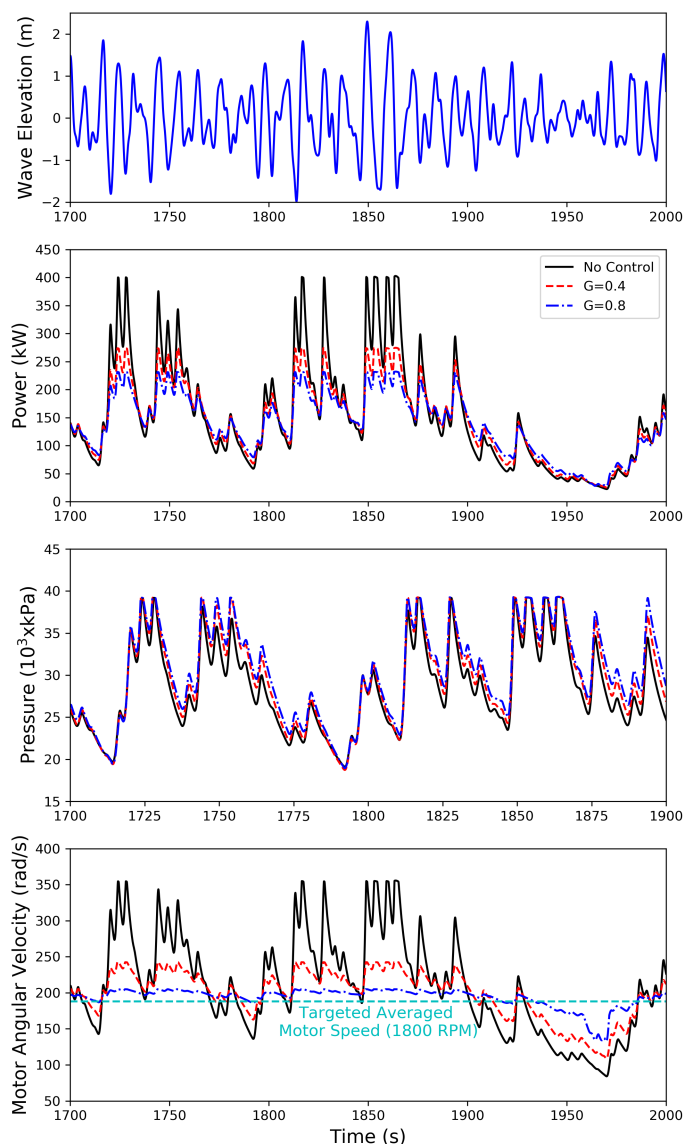

FIGURE 9. TIME HISTORIES OF THE WAVE ELEVATION, POWER OUTPUT, SYSTEM HYDRAULIC PRESSURE, AND HYDRAULIC MOTOR ANGULAR VELOCITY FOR IWS2 WITH DIFFERENT PROPORTIONAL GAIN

draulic pressure in the system, the power output fluctuation was decreased and the R_{PF} was reduced from 6.9 to 3.1, which came with an energy loss of 4%. Because the hydraulic PTO was designed for IWS2 and IWS5, the pressure bypass valve was found to be less effective for other off-design small energy sea states, such as IWS4. As shown in Fig. 8, the modeled system hydraulic pressure was significantly lower than the threshold limit, and the bypass valve was not activated for IWS4.

Power-Based Setpoint Control

A pressure bypass valve is effective at reducing power spikes. However, too much energy is released if the value of the threshold limit is too low. Here, we used the power-based
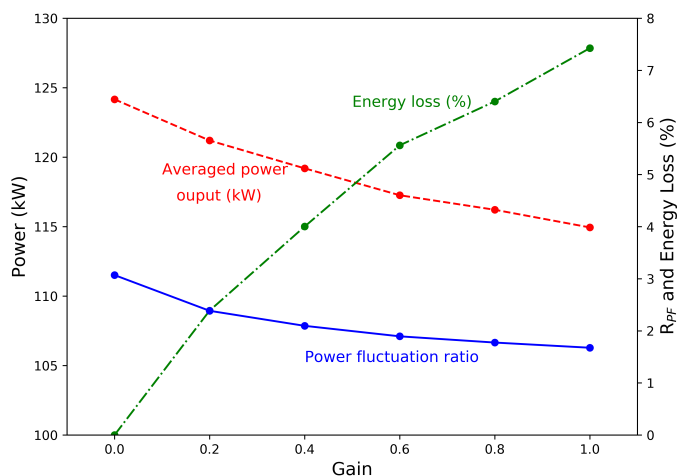
7

FIGURE 10. INFLUENCE OF CHANGING THE PROPORTIONAL GAIN FOR THE CONTROLLER ON POWER SMOOTHING AND ENERGY LOSS

setpoint control method in an attempt to reduce the power fluctuation in an electric generator while maintaining the same level of power output. The effect of tuning the control parameter (i.e., proportional gain) to adjust WEC performance was analyzed for IWS2, as shown in Fig. 9.

Both the accumulator and pressure bypass valve were used for the simulated case, and the controller was applied to the generator by changing the instantaneous value for the rotational damper to adjust the applied torque to the system. Therefore, the controller was effective at reducing the power spike but had a very limited influence on the hydraulic pressure fluctuation. Note that the control method could be applied without the accumulator and pressure bypass valve, but we found the method to be more effective when both the accumulator and pressure bypass valve were applied. In addition, because we assumed a fixed hydraulic motor displacement, the setpoint control method also helped reduce the velocity fluctuation for the hydraulic motor, which could be critical for system reliability.

Figure 10 shows the influence of changing the proportional gain for the controller on power smoothing and energy loss. By increasing the proportional gain for the controller, the power output fluctuation was reduced. However, there were also some losses in power performance. Future analysis on the applications for different control targets, such as hydraulic pressure, hydraulic flow rate, and motor velocity, could be beneficial to the WEC PTO design optimization.

Overall Efficiency

To analyze the overall performance of the system as well as the efficiency of the applied power smoothing methods, we used an accumulator with a volume of 1 m^3, a pressure bypass valve with a pressure threshold of 3.45×10^4 kPa, and a proportional gain of 0.4 for the setpoint control method. The WEC performance was examined for all six sea states used in the Wave Energy Prize (Table 3), with and without applying the power
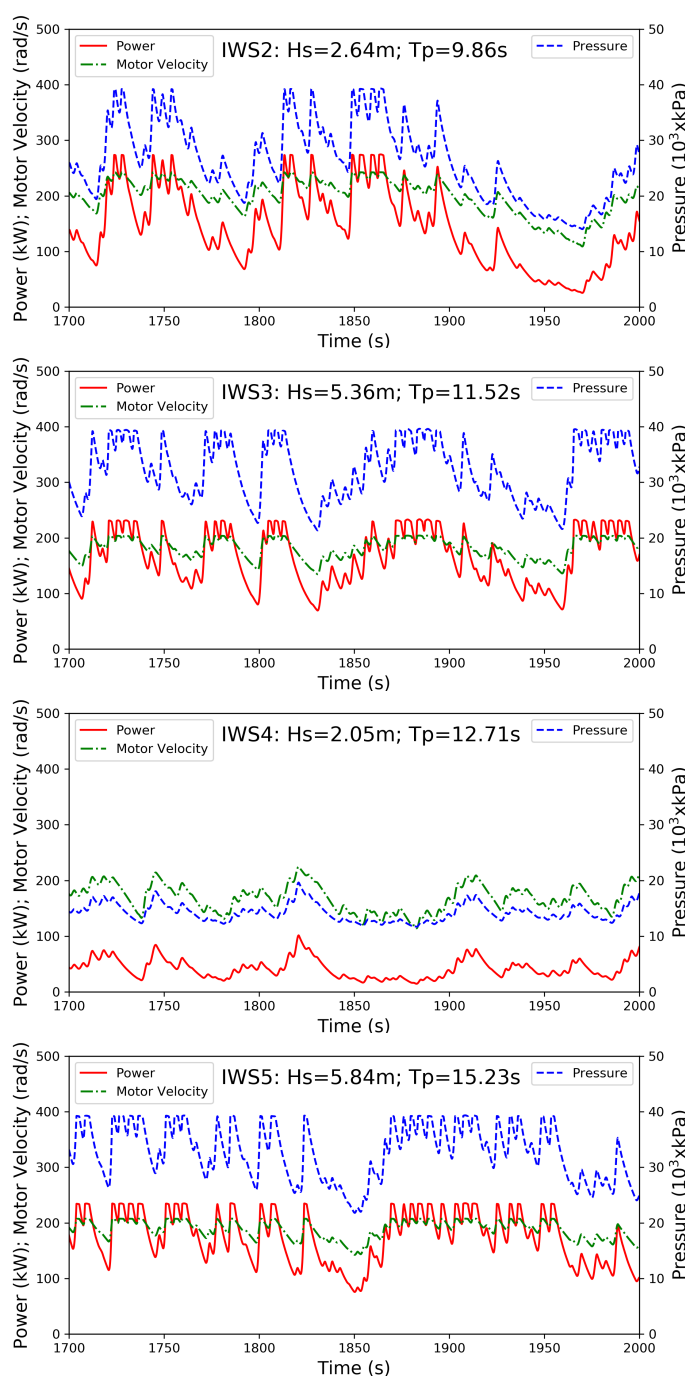

FIGURE 11. TIME HISTORIES OF THE POWER OUTPUT, SYSTEM HYDRAULIC PRESSURE AND MOTOR VELOCITY WHEN APPLYING THE POWER SMOOTHING METHODS.

smoothing methods. The results are listed in Table 5, and the time histories of the WEC-Sim simulations output for four selected sea states (IWS2-5) are presented in Fig. 11. The annual averaged energy production (AAEP) was calculated by multiplying P_E by the weighting function listed in Table 3. Note that the transmission losses and maintenance-related downtime losses were excluded.

8

TABLE 5. RM3 POWER PERFORMANCE WITH AND WITHOUT APPLYING THE POWER SMOOTHING METHODS

Wave #	Without Power Smoothing		With Power Smoothing	
	P_E (kW)	ΔP_E	P_E (kW)	ΔP_E
IWS 1	77	961	79	290
IWS 2	126	1321	119	250
IWS 3	338	3191	182	183
IWS 4	75	639	63	200
IWS 5	317	2485	173	185
IWS 6	124	910	100	262
AAEP	107	–	86	–
P_{rated}	3191	–	286	–

We here defined the largest P_{max} among all of the six sea states as the rated power, P_{rated}. As expected, the rated power and the fluctuation in power output were reduced significantly when the power smoothing methods were applied. This study demonstrated how we can practically design the PTO system by using these power smoothing methods to reduce the maximum power fluctuation, ΔP_E (IWS3), by one order of magnitude. By reducing spikes in power output, it also helps reduce the required size of the generator (i.e., rated power). Based on the selected parameters for the PTO subsystems and the power smoothing methods, the simulated FPA design has a capacity factor of 30.1%[3] and an AAEP of 86.2 kW. This verifies the quantity given by the RM project [8], which was calculated based on simplified assumptions. Note that we assumed a fixed hydraulic motor displacement with a targeted motor velocity and the PTO was designed to maximize the WEC power output for IWS2, the power performance for the WEC at other sea states could be improved. These power smoothing methods were more effective for sea states with a larger wave power (IWS3 and IWS5) and were not tuned for those off-design, less-energetic wave conditions. It is anticipated that a larger accumulator or other type of energy storage units (e.g., battery) can be applied to further mitigate the variation if it is cost-effective.

DISCUSSION

Reducing the power fluctuation has a direct impact on the potential LCOE. The peak generator rating is typically determined by the power output in relation to run time and load profile. Being that the run time is relatively short for the peak wave conditions, the generator is likely not going to be designed for the instantaneous peak, but reducing this peak will result in generator cost reductions. For simplicity, we determined

the peak generator rating using the statistically calculated peak power from the simulation. On the other hand, the average power produced by the generator dictates the potential revenue stream of the WEC. Putting this in terms of LCOE, reducing the peak-to-average power ratio can lower the system capital expenditure while maintaining annual energy production. With that being said, it is important to consider that the PTO portion of the capital expenditure is not directly proportional to the peak power, particularly for hydraulic systems like those studied here. The additional components used in this study to retstrain pressure and peak power would add to PTO cost compared to a system that does not have them, but can reduce the overall cost of the PTO. This is because they reduce generator size and the need for more costly high pressure components. Additionally, by reducing the peak-to-average ratio, the gear speed of the generator and the hydraulic motor are closer to steady-state operation, which helps reduce mechanical and volumetric losses.

As shown by the simulation results, there is more benefit to this system in higher energetic sea states. The PTO in this study incorporates a linear, dual-acting piston to couple to the WEC. Sizing this piston can be very challenging when using fixed displacement motors and no internal storage, because there is a trade-off between the maximum PTO pressure and the size of the piston. Large diameter and stroke hydraulic cylinders are more expensive, not only because of the material requirements, but because maintaining tolerances at longer stroke lengths becomes increasingly more challenging. However, smaller displacement cylinders require larger design pressures to produce the same power as a larger displacement cylinder, and increasing system cost in return. While not directly studied here, this indicates that there may be benefit to exploring the conversion efficiency trade offs associated with variable displacement hydraulic motors to maintain a desirable generator speed and improve performance in less energetic sea states.

CONCLUSIONS

A detailed hydraulic PTO model was developed and applied to evaluate the PTO efficiency and the trade-off between the average power output and the fluctuation over time using different power smoothing methods. This included a pressure accumulator for energy storage, a pressure bypass valve for removing the pressure and power generation spikes, and a power-based set-point controller. In general, we found that the pressure accumulator is effective at reducing the small power/pressure fluctuation. The pressure relief valve is necessary to remove the large spikes. The power-based setpoint controller is helpful for reducing peak power with limited energy losses and is effective at regulating the angular velocity for the motor. The study also demonstrated how we can practically design the PTO system by using these power smoothing methods to reduce the maximum power fluctuation by one order of magnitude and verified the PTO design specifications and power performance efficiency shown in the RM project. As shown by the simulation results, there is more benefit to the system in higher energetic sea states when these power

---

[3]If the largest P_E (instead of P_{max}) among all of the six sea states was used to define the rated power, the capacity factor is equal to 47.4%.

smoothing methods are applied. The advantage also comes from the fact that there is a significant amount of energy being released at those sea states. Overall, it is possible to obtain a power output that is closer to steady-state operation, which will minimize the voltage and frequency fluctuation and the impact to the grid system. However, as quantified in this study, there is a trade-off between the power output and fluctuation and will have a direct impact on the potential LCOE.

In this study, the selection of the PTO parameters is suboptimal. All of the above-mentioned PTO design trade-offs are important considerations when attempting to minimize LCOE, but they are also interdependent. Therefore, to fully quantify the benefit that this configuration may have on LCOE, a detailed cost trade off study would need to be performed. Further investigation could also include a PTO design optimization study, particularly associated with PTO capacity factor, off-design efficiency improvement, variable displacement motor application, and additional energy costs related to the hydraulic system.

REFERENCES
[1] Gunn, K., and Stock-Williams, C., 2012. "Quantifying the global wave power resource," *Renewable Energy, 44*, pp. 296–304.
[2] Falcão, A. F. D. O., 2010. "Wave Energy Utilization: A Review of the Technologies," *Renewable and Sustainable Energy Reviews, 14*, pp. 899–918.
[3] Jenne, D. S., Yu, Y.-H., and Neary, V., 2015. "Levelized Cost of Energy Analysis of Marine and Hydrokinetic Reference Models," In 3rd Marine Energy Technology Symposium, Washington, D.C., United States.
[4] Muljadi, E., and Yu, Y.-H., 2015. "Review of Marine Hydrokinetic Power Generation and Power Plant," *Electric Power Components and Systems, 43*(12), pp. 1422–1433.
[5] Tedeschi, E., Carraro, M., Molinas, M., and Mattavelli, P., 2011. "Effect of control strategies and power take-off efficiency on the power capture from sea waves," *IEEE Transactions on Energy Conversion, 26*(4), pp. 1088–1098.
[6] Salter, S. H., Taylor, J. R. M., and Caldwell, N. J., 2002. "Power conversion mechanisms for wave energy," *Proceedings of the Institution of Mechanical Engineers, Part M: Journal of Engineering for the Maritime Environment, 216*(1), pp. 1–27.
[7] Cruz, J., 2008. *Ocean Wave Energy: Current Status and Future Perspectives*. Springer Verlag.
[8] Neary, V. S., Previsic, M., Jepsen, R. A., Lawson, M. J., Yu, Y.-H., Copping, A. E., Fontaine, A. A., Hallett, K. C., and Murray, D. K., 2014. Methodology for Design and Economic Analysis of Marine Energy Conversion (MEC) Technologies, Sandia National Laboratories, Albuquerque, NM.
[9] So, R., Simmons, A., Brekken, T., Ruehl, K., and Michelen, C., 2015. "Development of PTO-Sim A power performance module for the open-source wave energy converter code WEC-Sim," *34th International Conference on Ocean, Offshore and Arctic Engineering*.
[10] Yu, Y.-H., Lawson, M., Ruehl, K., and Michelen, C., 2014. "Development and Demonstration of the WEC-Sim Wave Energy Converter Simulation Tool," In 2nd Marine Energy Technology Symposium, Seattle, WA.
[11] Cummins, W., 1962. The Impulse Response Function and Ship Motions, David Taylor Model Dasin (DTNSRDC).
[12] Lee, C., and Newman, J., 2015. WAMIT User Manual Version 7.1.
[13] Yu, Y., Lawson, M., Li, Y., Previsic, M., Epler, J., and Lou, J., 2015. Experimental Wave Tank Test for Reference Model 3 Floating-Point Absorber Wave Energy Converter Project, National Renewable Energy Laboratory (NREL), Golden, CO.
[14] Bull, D., and Dallman, A. R., 2017. "Wave Energy Prize Experimental Sea States Selection," In 36th International Conference on Ocean, Offshore and Arctic Engineering, Trondheim, Norway.

10